Proc. Natl. Acad. Sci. USA
Vol. 93, pp. 4051–4056, April 1996
Medical Sciences

Immunologic basis of transplant-associated arteriosclerosis

(mutant mice/homologous recombination/immune deficiency/allogeneic vascular transplantation)

CHENGWEI SHI*, WEN-SEN LEE*, QI HE*†, DOROTHY ZHANG*, DONALD L. FLETCHER, JR.*, JOHN B. NEWELL‡, AND EDGAR HABER*§

*Cardiovascular Biology Laboratory, Harvard School of Public Health, 677 Huntington Avenue, Boston, MA 02115; and ‡Cardiac Computer Center, Massachusetts General Hospital, Boston, MA 02114

Communicated by Alexander Rich, Massachusetts Institute of Technology, Cambridge, MA, December 27, 1995

ABSTRACT **Although immunosuppressive therapy minimizes the risk of graft failure due to acute rejection, transplant-associated arteriosclerosis of the coronary arteries remains a significant obstacle to the long-term survival of heart transplant recipients. The participation of specific inflammatory cell types in the genesis of this lesion was examined in a mouse model in which carotid arteries were transplanted across multiple histocompatibility barriers into seven mutant strains with immunologic defects. An acquired immune response—with the participation of CD4$^+$ (helper) T cells, humoral antibody, and macrophages—was essential to the development of the concentric neointimal proliferation and luminal narrowing characteristic of transplant arteriosclerosis. CD8$^+$ (cytotoxic) T cells and natural killer cells were not involved in the process. Arteries allografted into mice deficient in both T-cell receptors and humoral antibody showed almost no neointimal proliferation, whereas those grafted into mice deficient only in helper T cells, humoral antibody, or macrophages developed small neointimas. These small neointimas and the large neointimas of arteries grafted into control animals contained a similar number of inflammatory cells; however, smooth muscle cell number and collagen deposition were diminished in the small neointimas. Also, the degree of inflammatory reaction in the adventitia did not correlate with the size of the neointima. Thus, the reduction in neointimal size in arteries allografted into mice deficient in helper T cells, humoral antibody, or macrophages may be accounted for by a decrease in smooth muscle cell migration or proliferation.**

Transplant-associated arteriosclerosis is the major cause of cardiac allograft failure and consequent mortality after the first postoperative year (1), and it appears to be a significant problem in the long-term survival of kidney transplants (2). In contrast with common arteriosclerosis, the lesion associated with transplant arteriosclerosis involves the artery in a concentric rather than eccentric fashion and often extends beyond the epicardial coronary arteries to the secondary and tertiary intramyocardial branches (3). Lipid accumulation is less common in the early development of the transplant-associated lesion (4), and the tempo of the disease is faster (2). Inflammatory cells infiltrate the blood vessels of the transplanted organ (5) and produce cytokines, growth factors, and chemotactic agents (6–8) that have been suggested to cause vascular smooth muscle cell proliferation, a cardinal feature of the mature arteriosclerotic lesion (9). Although the complexity of the transplant-associated lesion and the many cell types involved—as well as the likely participation of a variety of growth factors and cytokines—suggest stimulation by an immune mechanism, it has not been possible to assign a pathogenic mechanism to the disease. To study the specific components of the immune response in transplant arteriosclerosis and the relative importance of the inflammatory cell types involved, we applied a model for quantitatively evaluating vascular lesions after carotid artery allotransplantation (9) to seven mutant mouse strains with immunologic defects.

EXPERIMENTAL PROCEDURES

Animals. B10.A(2R) (*H-2^{h2}*) mice were used as donors. Table 1 lists the mutant mouse strains used as recipients. Mice were obtained from The Jackson Laboratories unless indicated otherwise in the table legend. For each mutant strain, a marked reduction in the number of the cell type in question was confirmed either by fluorescence-activated cell sorting in peripheral blood or by immunohistochemical examination of the spleen or the carotid artery transplant. For the mice with no acquired immune response (*Rag-2$^-$*), reductions in the number of B cells, CD4$^+$ T cells, and CD8$^+$ T cells were confirmed.

Transplantation. A donor carotid artery segment was attached in a loop onto the carotid artery of a histoincompatible recipient (9). In brief, the operation was performed on anesthetized mice under a dissecting microscope (model M3Z; Wild, Heerbrugg, Switzerland). A midline incision was made on the ventral side of the neck from the suprasternal notch to the chin. The left carotid artery was dissected from the bifurcation in the distal end toward the proximal end as far as was technically possible. The artery was then occluded with two microvascular clamps (8 mm long; Roboz Surgical Instruments, Rockville, MD), one at each end, and two longitudinal arteriotomies (0.5–0.6 mm) were made with a fine needle (30 gauge) and scissors. In the donor mouse both the left and the right carotid arteries were fully dissected from the arch to the bifurcation. The graft was then transplanted paratopically into the recipient in an end-to-side anastomosis with an 11/0 continuous nylon suture under ×16 or ×25 magnification, and the skin incision was closed with a 4/0 interrupted suture. The time during which the graft was ischemic did not exceed 60 min. Grafts were harvested 30 days after transplantation, a point at which a fully developed, nearly occlusive lesion had been observed in B10.A(2R) (*H-2^{h2}*) to C57BL/6J (*H-2^b*) mouse carotid artery transplantations (9).

Histology and Morphometry. The proximal half of the transplanted loop (about 2.5 mm) was fixed overnight in methyl Carnoy's fixative at 4°C and embedded in paraffin, and the other half was fixed in 4% paraformaldehyde for 3 h, dehydrated in 30% sucrose for 48 h, embedded in medium (OCT compound; Miles), and then frozen in powdered dry ice. Histologic sectioning was begun at the center of the graft to avoid effects of the suture line. Tissue samples in methyl Carnoy's fixative were stained with α-actin or CD45 antibody,

The publication costs of this article were defrayed in part by page charge payment. This article must therefore be hereby marked "*advertisement*" in accordance with 18 U.S.C. §1734 solely to indicate this fact.

Abbreviation: MHC, major histocompatibility complex.

†Present address: Department of Molecular and Cellular Biology, Harvard University, 7 Divinity Avenue, Cambridge, MA 02138.
§To whom reprint requests should be addressed.

Table 1. Mouse strains used as recipients for carotid artery allografts from B10.A(2R) *H-2^{h2}* donors

Mutant	Defect	Strain designation	Control and haplotype
Rag-2$^{-/-}$; V(D)J recombinase gene disrupted (10); recombinase enzyme absent	No antigen-specific cellular and humoral immune response	TIM *Rag-2** (Fig. 1*A*)	B6129F$_2$/J *H-2^b* (Fig. 1*D*)
μMT$^{-/-}$; gene for a membrane exon of IgM μ chain disrupted (11); IgM receptor on pre-B cells absent	B cells depleted and humoral immune response deficient	MμMT$^+$ (Fig. 1*B*)	B6129F$_2$/J *H-2^b* (Fig. 1*D*)
CD4$^{-/-}$; CD4 gene disrupted (12)	CD4$^+$ T cells absent	CD4^{tm1Knw} (Fig. 1*C*)	B6129F$_2$/J *H-2^b* (Fig. 1*D*)
MHC II$^{-/-}$; MHC class II *H-2A$^b_\beta$* gene disrupted (13)	CD4$^+$ T cells depleted	C2D‡ (Fig. 1*E*)	C57BL/6J *H-2^b* (Fig. 1*H*)
MHC I$^{-/-}$; β_2-microglobulin gene disrupted (14)	CD8$^+$ T cells depleted	C57BL/6J-*b2m^{m1Unc}* (Fig. 1*F*)	C57BL/6J *H-2^b* (Fig. 1*H*)
bg^J/bg^J (beige) (15)	Natural killer cells depleted	C57BL/6J-*bg^J* (Fig. 1*G*)	C57BL/6J *H-2^b* (Fig. 1*H*)
op/op (osteopetrosis) (16)	Macrophage colony stimulating factor and macrophages depleted	B6C3Fe-*a/a-op* (Fig. 1*I*)	B6C3Fe-*a/a+/op H-2$^{k/b}$* (Fig. 1*J*)

Mice were obtained from The Jackson Laboratories, except as noted. MHC, major histocompatibility complex.
*Provided by Frederick W. Alt, The Children's Hospital, Boston. Strain is available from GenPharm (Mountain View, CA).
†Obtained by permission of Klaus Rajewsky, Institute of Genetics, University of Cologne. Strain is maintained by The Jackson Laboratories.
‡Obtained from GenPharm.

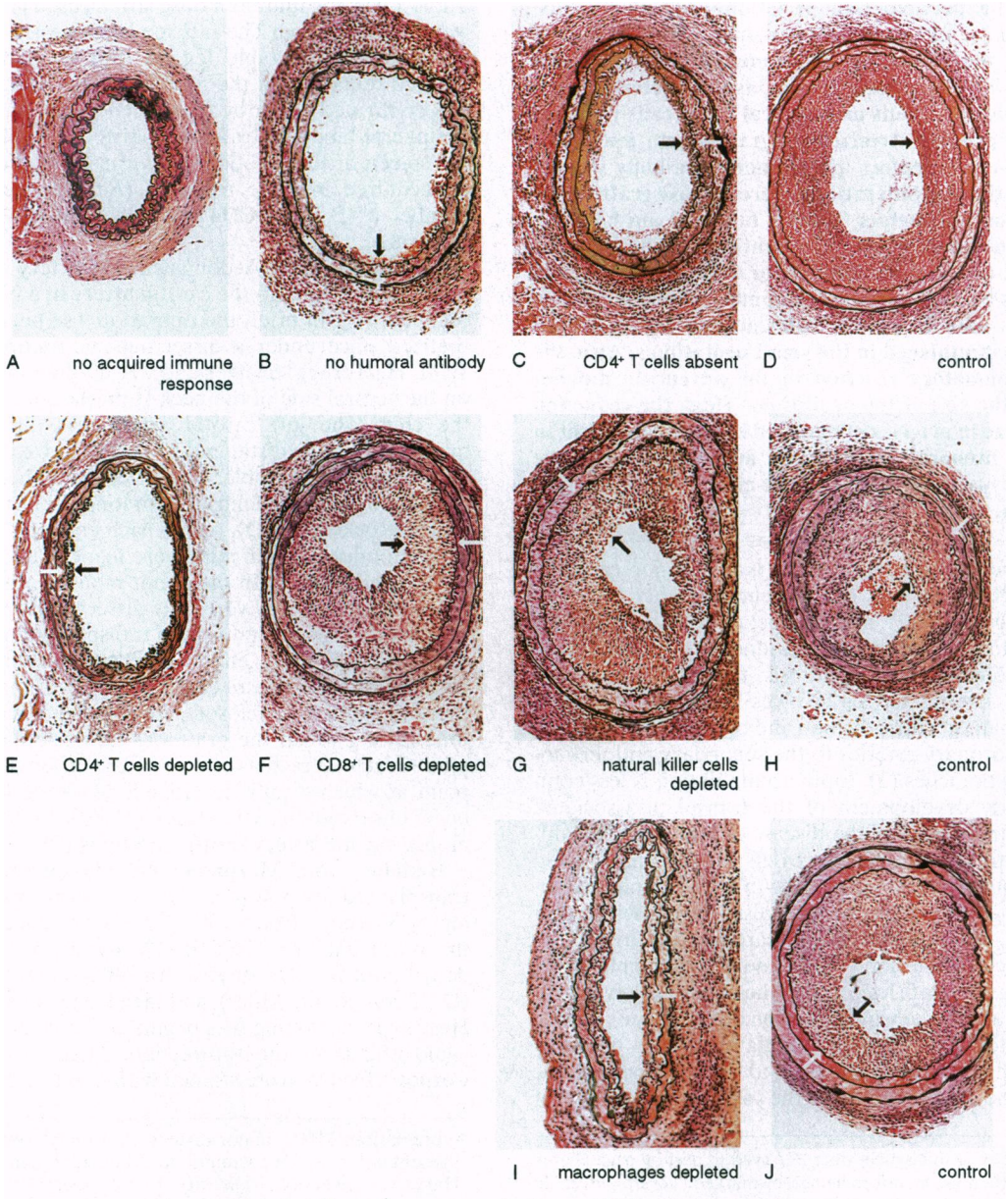

FIG. 1. *(Legend appears at the bottom of the opposite page.)*

and the paraformaldehyde-fixed frozen specimens were cut in a cryotome and immunostained with CD4, CD8, or Mac-1 antibody (9). Histologic, morphometric, and immunocytochemical analyses were performed as described (9).

The areas of the neointima and the media were measured by computerized planimetry on sections treated with Verhoeff's stain as described (9). On serial section, intimal lesions were generally uniform from the center of the carotid artery loop to ≈720 μm; measurements were obtained from sections taken 150 μm from the center of the loop (means from 4 to 10 animals per group). To compensate for variations in vessel diameter among individual mice, the data were analyzed as a ratio of intimal area (I)/intimal + medial area ($I + M$) × 100. Smooth muscle cell number was estimated by subtracting the number of $CD45^+$ cells in the neointima from the total number of nuclei in the neointima. This estimation was supported by staining the smooth muscle cells with an antibody to smooth muscle α-actin.

Statistical Methods. After a Pearson χ^2 test of normality revealed that the raw $I/(I + M)$ morphometric ratios, cell counts, and areas were nonnormal in distribution for some of the groups, the logarithms of these ratios, counts, and areas were computed and the logarithmic values were each retested for normality. The log-transformed variables tested normal for all control and mutant animal groups. These transformed variables were then subjected to a univariate one-way analysis of variance (BMDP program P7D) (17) with contrasts to compare each mutant group with its appropriate control (seven comparisons per variable). All seven mutant groups and their three controls were tested together in estimating these correlations, providing a sample size of 30 (3 mice from each of the 10 groups). The overall analysis of variance was highly significant ($P < 0.0004$). Individual comparisons were considered significant if the P value was < 0.0071. This cutoff was required because we applied the Bonferroni correction for multiple comparisons (α cutoff P value for significance, 0.05/7 comparisons per variable = 0.0071).

To determine the relation between intimal area and adventitial inflammatory cell number and that between intimal smooth muscle cell number and adventitial inflammatory cell number, we subjected the two correlation coefficients, R, to Fisher's z test of the null hypothesis of zero correlation (18).

RESULTS

Intimal Area in Allografted Arterial Loops. We performed carotid artery transplantations in seven mutant mouse strains (Table 1). Arteriosclerotic lesions develop in the allografted arterial loop much as they do in transplanted human vessels—with early infiltration of inflammatory cells and late accumulation of smooth muscle cells—but at an accelerated pace: the neointima that forms in the mouse vessel becomes nearly occlusive within 30 days of transplantation. The area of the neointima on cross section, from the vessel lumen to the internal elastic lamina, indicates the degree of transplant arteriosclerosis (Fig. 1, between arrows in *B–J*, and Fig. 2).

Arteries allografted into mice in which one of the genes coding for immunoglobulin variable-(diversity)-joining [V(D)J] segment recombination activity (*Rag-2*) had been deleted (10) formed almost no neointima after 30 days (Fig. 1 *A* vs. *D*, and Fig. 2), indicating that an acquired immune response associated with an immunoglobulin or T-cell receptor gene rearrangement was required for the genesis of transplant arteriosclerosis. A minimal neointima was also manifest in arteries allografted into mice that carry a mutated exon in the gene (μM) encoding the membrane form of the immunoglobulin μ chain, a disruption that arrests B-cell development at the pre-B-cell stage without impairing T-cell development (11); the μM mutation is designated μMT (Fig. 1 *B* vs. *D*, and Fig. 2). This impaired development of neointima may have been due either to the absence of the B-cell's ability to produce specific antibody or to the absence of its ability to act as an antigen-presenting cell.

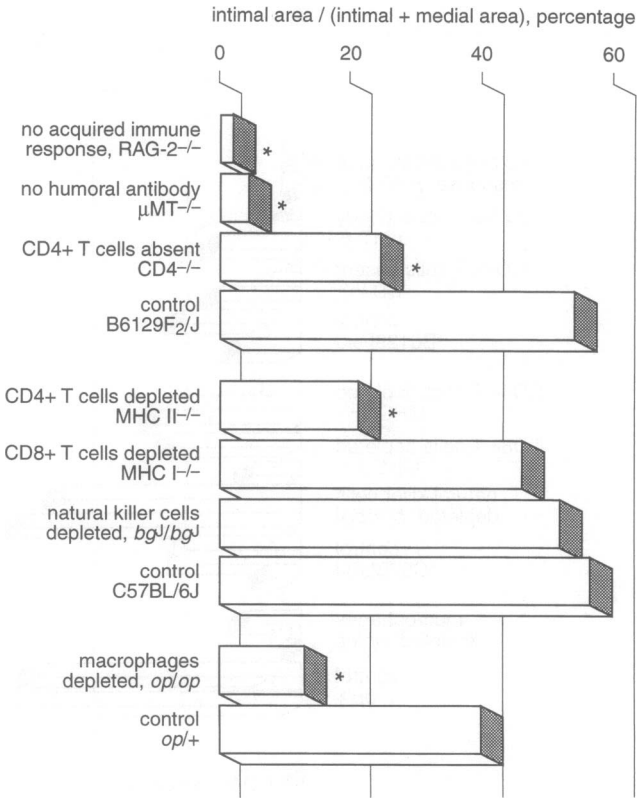

FIG. 2. Comparison of intimal areas [presented as a ratio of intimal area (I)/intimal + medial area ($I + M$) × 100] in mouse carotid artery allograft sections harvested 30 days after transplantation into the strains described in Table 1. *Rag-2*$^{-/-}$, $n = 10$; μMT$^{-/-}$, $n = 8$; CD4$^{-/-}$, $n = 7$; B6129F$_2$/J, $n = 6$; MHC II$^{-/-}$, $n = 4$; MHC I$^{-/-}$, $n = 8$; *bg*^{J}/*bg*^{J}, $n = 7$; C57BL/6J, $n = 7$; *op/op*, $n = 7$; *op/+*, $n = 5$. Asterisks mark values significantly lower than respective controls ($P < 0.0071$; see *Statistical Methods*): *Rag-2*$^{-/-}$, $P < 0.00005$; μMT$^{-/-}$, $P < 0.00005$; CD4$^{-/-}$, $P = 0.002$; MHC II$^{-/-}$, $P = 0.004$; *op/op*, $P = 0.002$.

T-cell maturation in the thymus depends on expression of the major histocompatibility complex (MHC) molecules. Disruption of the MHC class II gene $H\text{-}2A^b_\beta$ produces mice that are depleted of mature $CD4^+$ T cells (13), and disruption of the β_2-microglobulin gene produces mice deficient in MHC class I molecules and $CD8^+$ T cells (14). The gene coding for the CD4 molecule itself can also be disrupted (12). In arteries allografted into mice in which $CD4^+$ T cells were absent (CD4 gene disruption) or their number was reduced (MHC class II $H\text{-}2A^b_\beta$ gene disruption), the neointimal area was significantly smaller than that in controls (Fig. 1 *C* vs. *D* and *E* vs. *H*, respectively, and Fig. 2), whereas in arteries allografted into mice in which the number of $CD8^+$ T cells was reduced, the neointimal area did not differ from that in controls (Fig. 1 *F* vs. *H*, and Fig. 2).

Beige (*bg*^{J}) is a spontaneous recessive mutation on mouse chromosome 13 associated with an impairment in natural killer

FIG. 1. Selected sections from mouse carotid artery loops allografted by a method we described previously (9) into the strains listed in Table 1. The neointima extends between the internal elastic lamina [Verhoeff's elastin stain (9)] and the vessel lumen (between arrows in *B–J*; there is no neointima in *A*). *(A) Rag-2*$^{-/-}$. *(B)* μMT$^{-/-}$. *(C)* CD4$^{-/-}$. *(D)* B6129F$_2$/J control for *A–C*. *(E)* MHC II$^{-/-}$. *(F)* MHC I$^{-/-}$. *(G) bg*^{J}/*bg*^{J}. *(H)* C57BL/6J control for *E–G*. *(I) op/op*. *(J) op/+* control for *op/op*. (×150.)

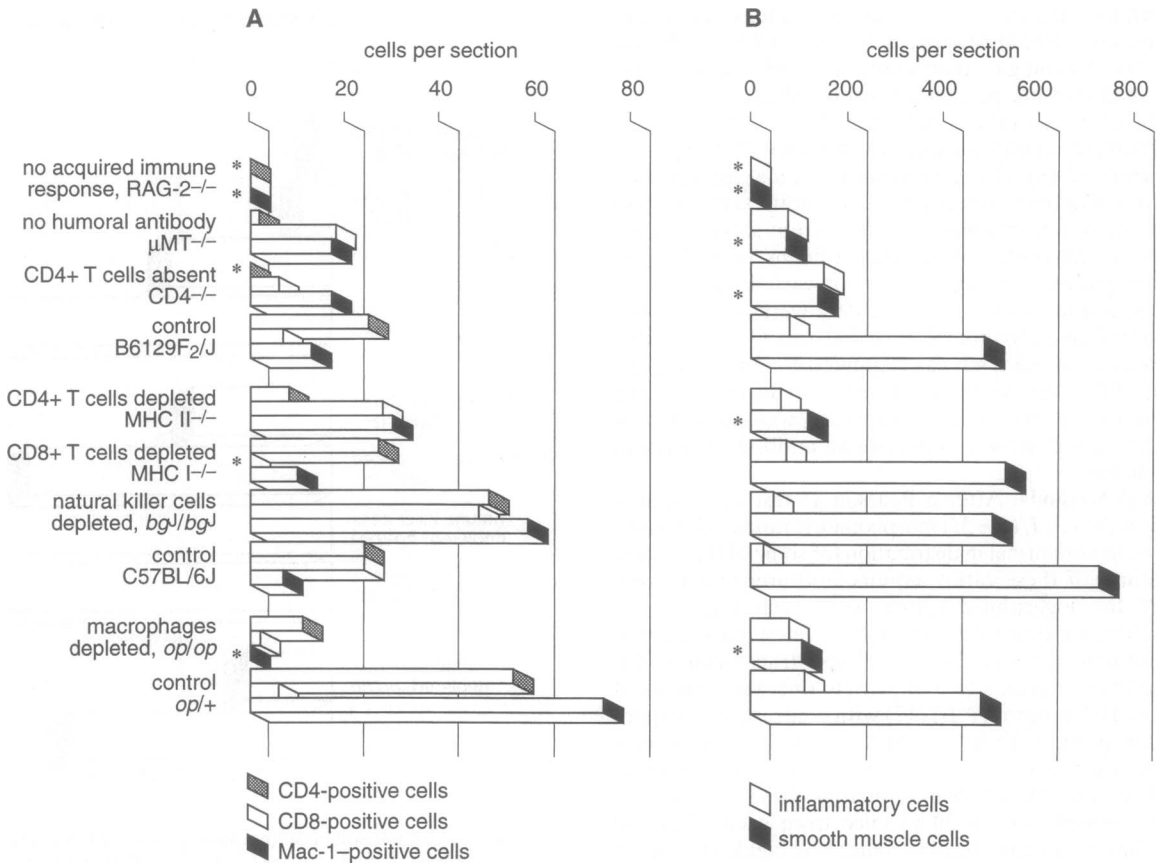

FIG. 3. *(A)* Neointimal CD4$^+$, CD8$^+$, and Mac-1$^+$ cells per section at 30 days after transplantation. Nuclei in three sections each from three animals were counted. Asterisks mark values significantly lower than respective controls ($P < 0.0071$, under *Experimental Methods*, see *Statistical Methods*): *Rag-2*$^{-/-}$ CD4$^+$, $P = 0.0004$; Mac-1$^+$, $P = 0.0006$; CD4$^{-/-}$ CD4$^+$, $P = 0.0004$; MHC I$^{-/-}$ CD8$^+$, $P = 0.0005$; *op/op* Mac-1$^+$, $P < 0.00005$. *(B)* Neointimal inflammatory cells (CD45$^+$) and smooth muscle cells (total nuclei minus number of CD45$^+$ cells) per section at 30 days. Nuclei in three sections each from three animals were counted. Asterisks mark values significantly lower than respective controls ($P < 0.0071$; see *Statistical Methods*): *Rag-2*$^{-/-}$ inflammatory, $P < 0.00005$; *Rag-2*$^{-/-}$ smooth muscle, $P < 0.00005$; μMT$^{-/-}$ smooth muscle, $P < 0.00005$; CD4$^{-/-}$ smooth muscle, $P < 0.00005$; MHC II$^{-/-}$ smooth muscle, $P < 0.00005$; *op/op* smooth muscle, $P = 0.001$.

cell function (15), although some investigators have observed diminished cytotoxic T-cell (19) and macrophage (20) activity as well. The neointimal area in arteries allografted into *bg*^{J} mice was not significantly different from that in controls (Fig. 1 *G* vs. *H*, and Fig. 2). Therefore, natural killer cells do not appear to be involved in the genesis of transplant-associated arteriosclerosis.

A spontaneous mutation in mice characterized by congenital osteopetrosis (*op/op*) is associated with a defect in macrophage differentiation (21) that causes a decrease in macrophage number. This defect is caused by a mutation in the coding region of the macrophage colony-stimulating factor gene (22). Arteries allografted into *op/op* mice developed a minimal neointima (Figs. 1*I* and 2), in contrast with those grafted into *op/+* animals (Figs. 1*J* and 2).

Characteristics of Significantly Reduced Neointima in Some Mutant Mice. Like their controls, arterial loops allografted into mice deficient in CD8$^+$ T cells (MHC I gene deletion) and natural killer cells (*bg/bg* mutant) developed extensive neointimas, whereas unlike their controls loops transplanted into mice deficient in the recombination-activating gene *Rag-2* developed almost no neointimas. In the remaining four experimental groups—mice deficient in CD4$^+$ T cells (MHC II and CD4 gene deletions), humoral antibody (μMT gene deletion), and macrophages (*op/op* mutant)—the transplanted loops developed neointimas smaller than those in controls. To delineate the mechanisms responsible for the persistence of a neointima, albeit smaller, in arterial loops transplanted into the *op/op* mice and MHC II, CD4, and μMT gene-deletion animals, we determined whether the cell type putatively absent in each of these four mutant recipients was present in the transplanted vessel, whether the cellular constitution of the reduced neointima differed from that of the fully developed neointima in controls, and whether we could show a difference in collagen deposition between arteries allografted into these four mutants and those grafted into their respective controls.

CD4$^+$ T cells were absent in arterial loops transplanted into the CD4 gene-deletion animals, and Mac-1$^+$ macrophages were absent in loops in the *op/op* animals in both the intima (Fig. 3*A*) and adventitia (data not shown). Thus we conclude that an intimal lesion can occur in the absence of CD4$^+$ T cells or Mac-1$^+$ macrophages. An alternative explanation for the relative reduction in formation of neointima would be the presence of one or more redundant mechanisms for cellular infiltration into the intima. In arteries allografted into the μMT gene-deletion mice, for example, the number of B cells in the peripheral blood constituted ≈2% that in controls as measured by fluorescence-activated cell sorting, although a few B cells were present in both the adventitia and the intima by immunohistology (data not shown). Because in this instance of a reduced neointima the gene deletion resulted in an absence of the IgM antigen receptor on pre-B-cells, it is possible that the small number of B cells revealed by fluorescence activated cell sorting represented cells that did not produce rearranged antibody.

Fig. 3*B* addresses the cellular composition of the smaller neointimas in arterial loops transplanted into the *op/op* mice

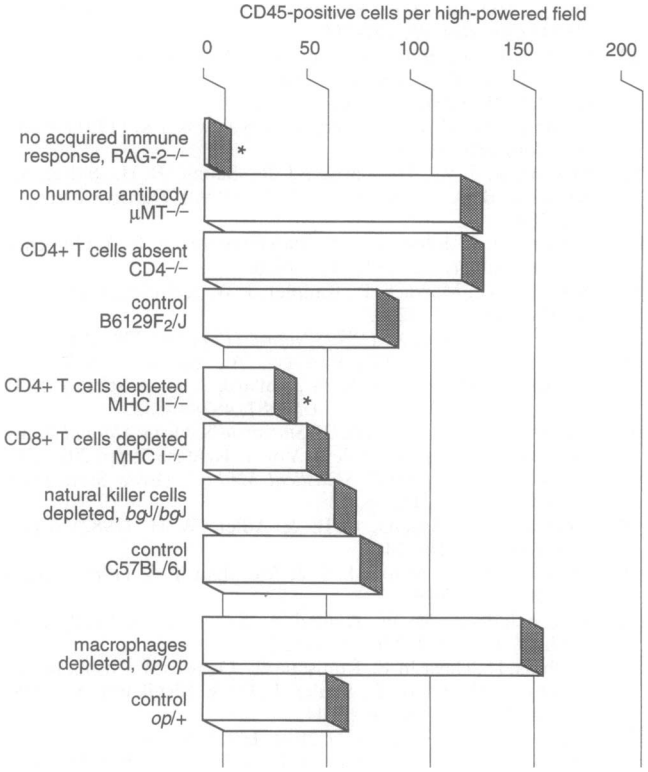

FIG. 4. Adventitial inflammatory cells ($CD45^+$) per section at 30 days after transplantation. Nuclei in three sections each from three animals were counted. Asterisks mark values significantly lower than respective controls ($P < 0.0071$; see *Statistical Methods*): *Rag-2*$^{-/-}$, $P < 0.00005$; MHC $II^{-/-}$, $P = 0.005$.

and MHC II, CD4, and μMT gene-deletion animals. In contrast with loops allografted into control mice and mutant mice (MHC I gene deletion and bg^J/bg^J mutant) that manifested large neointimas in which smooth muscle cells predominated at 30 days, the number of smooth muscle cells was reduced significantly in *op/op* mice and MHC II, CD4, and μMT gene-deletion mice. As there was no significant difference between leukocyte number (measured by CD45 staining) in the neointimas of loops transplanted into these four mutant recipients and leukocyte number in those of loops transplanted into controls, it appears that the absence of smooth muscle cell infiltration or proliferation was a major reason for the reduction in neointimal size in loops grafted into the *op/op* mice and MHC II, CD4, and μMT gene-deletion animals.

The large neointimas in arterial loops transplanted into control mice and MHC I gene deletion and bg^J/bg^J mice showed abundant collagen deposition between cells by the Masson trichrome stain, whereas the small neointimas in those transplanted into the *op/op* mice and MHC II, CD4, and μMT gene-deletion animals showed none (data not shown). Because smooth muscle cell number was diminished in these smaller neointimas, extracellular matrix, a product of smooth muscle cells, was apparently reduced.

Adventitial Inflammatory Reaction in Transplanted Arteries. Fig. 4 shows the number of $CD45^+$ cells in the adventitias of arterial loops transplanted into all seven mutant mice and their controls. With the exception of loops allografted into the *Rag-2-* and MHC II-deletion mice, the number of inflammatory cells in the adventitia did not differ significantly between mutants and controls and, most notably, between those other strains whose arterial loops had relatively reduced neointimas ($\mu MT^{-/-}$, $CD4^{-/-}$, and *op/op*) and their controls. These observations indicate that the degree of inflammatory reaction in the adventitia did not correlate with the size of the neointima (as assessed by area, $R = -0.14$, $P = 0.8$, not significant by the Fisher *z* test), and, particularly, that it did not correlate with the degree of smooth muscle proliferation in the neointima ($R = -0.075$, $P = 0.7$, not significant by the Fisher *z* test on a sample base of 30 sections).

DISCUSSION

In transplant-associated arteriosclerosis, inflammatory cells form a neointimal lesion in the donor arteries into which smooth muscle cells then migrate and proliferate. This process is distinguished from transplant rejection, which in its final manifestation is characterized by the killing of cells in the donor tissue (23). The experiments described here indicate first that the genesis of transplant arteriosclerosis depends on T-cell receptor and immunoglobulin gene rearrangement, which are both consequences of active immunization (Fig. 1*A* and Fig. 2, *Rag-2*$^{-/-}$). An antigen-independent immune response appears to be insufficient. Second, transplant arteriosclerosis develops independently of $CD8^+$ T cells and natural killer cells (Fig. 1*F* and *G*, and Fig. 2, MHC $I^{-/-}$ and bg^J/bg^J). Its development does appear to require the interaction of $CD4^+$ T cells, B cells, and macrophages; however, because deletion of any one of these cell types reduces the magnitude of the arteriosclerotic lesion greatly (Fig. 1 *B, C, E*, and *I*, and Fig. 2, $\mu MT^{-/-}$, $CD4^{-/-}$, MHC $II^{-/-}$, and *op/op*).

The presence of neointimal lesions in arterial loops transplanted into CD4 gene deletion and *op/op* mice, albeit smaller than those in controls, could not have been caused by a residuum of cells putatively absent in the mutant animals (i.e., leaky gene deletions) because $CD4^+$ T cells were not found in the $CD4^{-/-}$ group and Mac-1^+ macrophages were not found in the *op/op* group (Fig. 3*A*). Alternate pathways that involve other cell types are probably responsible for these smaller neointimas. We did observe a few B cells in arteries transplanted into mice depleted of humoral antibody (μMT gene deletion); however, this knockout is consistent with the presence of pre-B cells in which immunoglobulin gene rearrangement has not occurred. Thus, the presence of these B cells does not imply that the small neointimas in arterial loops allografted into $\mu MT^{-/-}$ mice were caused by allospecific antibody.

Our experiments also show that the extent of inflammatory cell infiltration—into the neointima as well as the adventitia of the transplanted vessel—does not correlate with the size of the neointimal lesion (Figs. 3*B* and 4) and consequent vascular stenosis; rather, the degree of smooth muscle cell migration or proliferation correlates with intimal size (Fig. 3*B*). Thus, the principal consequence of a reduction in the number of mature $CD4^+$ T cells and macrophages, and of the probable absence of allospecific antibody, appears to be inhibition of smooth muscle cell migration or proliferation (Fig. 3*B*).

The impaired smooth muscle cell proliferation (Fig. 3*B*) in mice deficient in $CD4^+$ T cells (MHC II and CD4 gene deletions), humoral antibody (μMT gene deletion), and macrophages (*op/op* mutant) could have resulted from the removal of a critical component in a sequential cascade of cytokine stimulation (24). This cascade would begin with $CD4^+$ T cells, which would in turn promote B-cell proliferation, humoral antibody production (25)—also implicated in another mouse model of allotransplantation (26), stimulation of macrophages by antibody through their Fcγ receptors (27), and, finally, elaboration by macrophages of growth factors such as fibroblast growth factor and platelet-derived growth factor (28). Were this pathway interrupted at any point in its course, reductions in levels of macrophage-produced fibroblast growth factors and platelet-derived growth factors would cause inhibition of smooth muscle cell migration or proliferation. Interruption of the pathway could be effected by the absence of a cytokine produced by a critical cell type in the chain or, alternatively, by the absence of positive feedback to $CD4^+$ T cells from B cells or macrophages through antigen presentation.

By studying this series of mutant mice deficient in a variety of inflammatory cell types, we have demonstrated that transplant-associated arteriosclerosis is a complex, multicellular process that depends on acquired immunity and requires mature $CD4^+$ T cells, B cells, and macrophages. Our observations are consistent with the identification of these cell types in the arteriosclerotic lesions of human transplant recipients (29). At a molecular level these data also suggest that MHC class II molecules and macrophage colony-stimulating factor are critical components of the cascade that leads to the development of arteriosclerosis. Because of the numerous combinations of genetically modified mice that can be studied in this model system, its power is not restricted to elucidating the cellular and molecular basis of transplant arteriosclerosis; the model should also prove useful in furthering the study of therapeutic interventions.

We thank Margaretha Doughty for careful management of the mouse colonies and Thomas McVarish for accomplished and perceptive editorial assistance. This work was supported by a grant from Bristol-Myers Squibb.

1. Sharples, L. D., Caine, N., Mullins, P., Scott, J. P., Solis, E., English, T. A., Large, S. R., Schofield, P. M. & Wallwork, J. (1991) *Transplantation* **52,** 244–252.
2. Paul, L. C. (1993) *Transplant. Proc.* **25,** 2024–2025.
3. Billingham, M. E. (1989) *Transplant. Proc.* **21,** 3665–3666.
4. Pucci, A. M., Clarke Forbes, R. D. & Billingham, M. E. (1990) *J. Heart Transplant.* **9,** 339–345.
5. Cramer, D. V., Wu, G. D., Chapman, F. A., Cajulis, E., Wang, H. K. & Makowka, L. (1992). *J. Heart Lung Transplant.* **11,** 458–466.
6. Russell, P. S., Chase, C. M., Winn, H. J. & Colvin, R. B. (1994) *Am. J. Pathol.* **144,** 260–274.
7. Russell, M. E., Adams, D. H., Wyner, L. R., Yamashita, Y., Halnon, N. J. & Karnovsky, M. J. (1993) *Proc. Natl. Acad. Sci. USA* **90,** 6086–6090.
8. Russell, M. E., Wallace, A. F., Hancock, W. W., Sayegh, M. H., Adams, D. H., Sibinga, N. E. S., Wyner, L. R. & Karnovsky, M. J. (1995) *Transplantation* **59,** 572–578.
9. Shi, C., Russell, M. E., Bianchi, C., Newell, J. B. & Haber, E. (1994) *Circ. Res.* **75,** 199–207.
10. Shinkai, Y., Rathbun, G., Lam, K.-P., Oltz, E. M., Stewart, V., Mendelsohn, M., Charron, J., Datta, M., Young, F., Stall, A. M. & Alt, F. W. (1992) *Cell* **68,** 855–867.
11. Kitamura, D., Roes, J., Kühn, R. & Rajewsky, K. (1991) *Nature (London)* **350,** 423–426.
12. McCarrick, J. W., III, Parnes, J. R., Seong, R. H., Solter, D., Knowles, B. B. & McCarrick, J. W. (1993) *Transgenic Res.* **2,** 183–190.
13. Grusby, M. J., Johnson, R. S., Papaioannou, V. E. & Glimcher, L. H. (1991) *Science* **253,** 1417–1420.
14. Koller, B. H., Marrack, P., Kappler, J. W. & Smithies, O. (1990) *Science* **248,** 1227–1230.
15. Roder, J. & Duwe, A. (1979) *Nature (London)* **278,** 451–453.
16. Wiktor-Jedrzejczak, W., Bartocci, A., Ferrante, A. W., Jr., Ahmed-Ansari, A., Sell, K. W., Pollard, J. W. & Stanley, E. R. (1990) *Proc. Natl. Acad. Sci. USA* **87,** 4828–4832.
17. Dixon, W. J., ed. (1992) *BMDP Statistical Software Manual* (Univ. of California Press, Berkeley), Vol. 1, Release 7, pp. 201–226.
18. Snedecor, G. W. (1967) *Statistical Methods* (Iowa State Univ. Press, Ames), 6th Ed., p. 185.
19. Saxena, R. K., Saxena, Q. B. & Adler, W. H. (1982) *Nature (London)* **295,** 240–241.
20. Mahoney, K. H., Morse, S. S. & Morahan, P. S. (1980) *Cancer Res.* **40,** 3934–3939.
21. Wiktor-Jedrzejczak, W., Ahmed, A., Szczylik, C. & Skelly, R. R. (1982) *J. Exp. Med.* **156,** 1516–1527.
22. Yoshida, H., Hayashi, S., Kunisada, T., Ogawa, M., Nishikawa, S., Okamura, H., Sudo, T., Shultz, L. D. & Nishikawa, S. (1990) *Nature (London)* **345,** 442–444.
23. Mandel, T. E. (1992) *Med. J. Aust.* **157,** 126–131.
24. Mosmann, T. R. & Coffman, R. L. (1989) *Annu. Rev. Immunol.* **7,** 145–173.
25. Lanzavecchia, A. (1990) *Annu. Rev. Immunol.* **8,** 773–793.
26. Russell, P. S., Chase, C. M., Winn, H. J. & Colvin, R. B. (1994) *J. Immunol.* **152,** 5135–5141.
27. Takai, T., Li, M., Sylvestre, D., Clynes, R. & Ravetch, J. V. (1994) *Cell* **76,** 519–529.
28. Ross, R. (1993) *Nature (London)* **362,** 801–809.
29. Hruban, R. H., Beschorner, W. E., Baumgartner, W. A., Augustine, S. M., Ren, H., Reitz, B. A. & Hutchins, G. M. (1990) *Am. J. Pathol.* **137,** 871–882.